

9. R. Steitz *et al.*, *Langmuir* **19**, 2409 (2003).
10. T. R. Jensen *et al.*, *Phys. Rev. Lett.* **90**(8), 86101 (2003).
11. A. Wallqvist, B. J. Berne, *J. Phys. Chem.* **99**, 2893 (1995).
12. A. Wallqvist, B. J. Berne, *J. Phys. Chem.* **99**, 2885 (1995).
13. K. Leung, A. Luzar, *J. Chem. Phys.* **113**, 5845 (2000).
14. K. Leung, A. Luzar, D. Bratko, *Phys. Rev. Lett.* **90**, 65502 (2003).
15. M. E. Paulaitis, L. R. Pratt, *Adv. Protein Chem.* **62**, 283 (2002).
16. L. R. Pratt, *Annu. Rev. Phys. Chem.* **53**, 409 (2002).
17. G. Hummer, S. Garde, A. E. Garcia, L. R. Pratt, *Chem. Phys.* **258**, 349 (2000).
18. K. Lum, A. Luzar, *Phys. Rev. E.* **56**, R6283 (1997).
19. D. M. Huang, D. Chandler, *Proc. Natl. Acad. Sci. U.S.A.* **97**, 8324 (2000).
20. P. R. ten Wolde, D. Chandler, *Proc. Natl. Acad. Sci. U.S.A.* **99**, 6539 (2002).
21. K. Lum, D. Chandler, *Int. J. Thermophys.* **19**, 845 (1998).
22. R. D. Mountain, D. Thirumalai, *J. Am. Chem. Soc.* **125**, 1950 (2003).
23. R. Zhou, B. D. Silverman, A. Royyuru, P. Athma, *Proteins* **52**, 561 (2003).
24. The starting structure is taken from the crystal structure deposited in PDB (entry 1dhy.pdb). The interdomain distance of the crystal structure is increased by  $D$  along the direction of two domain centers of geometry to create "gaps" between the two domains (to make room for water). Various distances ranging from  $D = 2.5 \text{ \AA}$  to  $20.0 \text{ \AA}$  are studied. The resulting protein configurations are then solvated in a water box, with water layers at least  $8 \text{ \AA}$  from the protein surfaces. Figure 1 shows one such solvated configuration. Eight  $\text{Na}^+$  counterions are added to make the system electrically neutral. The solvated protein systems have up to 42,000 atoms (the actual size varies for different interdomain distances). The GROMACS simulation package is used here for this large system because of its fast speed (25). Each NPT MD simulation [(26), 1 atm and 300 K] is run in parallel with 8 to 16 processors on IBM SP2-Power3-375 MHz clusters. The OPLSAA force field is used for the protein (27), and a simple point charge (SPC) water model is used for the explicit solvent. For the long-range electrostatic interactions, the particle-mesh Ewald method is used. For the van der Waals interactions, a typical  $10 \text{ \AA}$  cutoff is used. A time step of  $2.0 \text{ fs}$  is used with bond lengths constrained. A standard equilibration procedure, which includes a conjugate gradient minimization and a 100-ps MD simulation with position restraints, is followed to equilibrate each solvated system. The final configurations from equilibration are then used for data collection. We have modified GROMACS to allow us to selectively turn off certain terms in the force field, in particular, the protein-water electrostatic potential, the attractive part of the protein-water van der Waals potential, the domain-domain electrostatic potential, and the attractive part of the domain-domain van der Waals potential. This approach allows us to make a sensitivity analysis of hydrophobic collapse and to compare the protein collapse with what is already known about the hydrophobic collapse of the plates.
25. E. Lindahl, B. Hess, D. van der Spoel, *J. Mol. Model.* **7**, 306 (2001).
26. One caveat is that NPT MD introduces fictitious dynamics from both the temperature and pressure control. New fictitious degrees of freedom are introduced, with corresponding kinetic energies, fictitious masses, and fictitious frequencies. These influence the time scales and can affect the rate processes observed. Nevertheless, the thermodynamic equilibrium water densities inside the interplate or interdomain region and the water depletion or dewetting phenomena should stay the same. Our observations about kinetics are borne out in careful studies.
27. W. L. Jorgensen, D. Maxwell, J. Tirado-Rives, *J. Am. Chem. Soc.* **118**, 11225 (1996).
28. The original total interdomain distance is about  $18.8 \text{ \AA}$ , so after the enlargement, the total interdomain distance is about  $22.8 \text{ \AA}$ . For simplicity, we will refer to it as interdomain gap distance  $D = 4 \text{ \AA}$  in the following.
29. It is tricky to define the water density inside the domain gap region, particularly for cases with very small  $D$  values, because the fluctuation in the number of water molecules can be fairly large compared with the total number of water molecules inside the region. In general, it is very difficult to directly measure the volume inside the domain gap region because of the irregularity of the protein domain structures; thus, we used a comparative way to measure the water density.
30. Y. Cheng, P. J. Rossky, *Nature* **392**, 696 (1998).
31. H. S. Ashbaugh, M. E. Paulaitis, *J. Am. Chem. Soc.* **123**, 10721 (2001).
32. Single-letter abbreviations for the amino acid residues are as follows: A, Ala; C, Cys; D, Asp; E, Glu; F, Phe; G, Gly; H, His; I, Ile; K, Lys; L, Leu; M, Met; N, Asn; P, Pro; Q, Gln; R, Arg; S, Ser; T, Thr; V, Val; W, Trp; and Y, Tyr.
33. This work was partially supported by a grant to B.J.B. from NIH (GM4330) and a Shared University Research (SUR) grant from the IBM Corporation to Columbia University.

7 June 2004; accepted 20 August 2004

# Climate Impact on Plankton Ecosystems in the Northeast Atlantic

Anthony J. Richardson<sup>1\*</sup> and David S. Schoeman<sup>2</sup>

It is now widely accepted that global warming is occurring, yet its effects on the world's largest ecosystem, the marine pelagic realm, are largely unknown. We show that sea surface warming in the Northeast Atlantic is accompanied by increasing phytoplankton abundance in cooler regions and decreasing phytoplankton abundance in warmer regions. This impact propagates up the food web (bottom-up control) through copepod herbivores to zooplankton carnivores because of tight trophic coupling. Future warming is therefore likely to alter the spatial distribution of primary and secondary pelagic production, affecting ecosystem services and placing additional stress on already-depleted fish and mammal populations.

Not only do plankton provide food for marine mammals and commercially important fish, they also play a fundamental role in the functioning of marine ecosystems by providing half the global primary production (1) and contributing substantially to biogeochemical cycling (2). How global climate change might affect biological communities such as marine plankton is therefore a matter for concern (3). There is evidence of climate-mediated biogeographical shifts among some groups of marine plankton such as the calanoid copepods (4), but the overall response of phytoplankton and zooplankton communities, which is likely to depend on the form and strength of the linkages between successive trophic levels, is not known. Until we understand these processes, we will not know how resilient such food webs are to global-scale impacts, such as climate change, eutrophication, pollution, or over-fishing, and it will be difficult to manage marine resources sustainably.

To predict the response of the base of the marine food web to climate change, we need a better understanding of the type and degree

of coupling between trophic levels in marine systems. Complex biological systems are generally controlled by their top predators through top-down control, by their producers through bottom-up control, or by a number of key species in the middle through wasp-waist control (5). For the plankton ecosystem within the marine pelagic realm, there is currently conflicting evidence on when these types of control operate, and on what scales. Some workers suggest tight bottom-up coupling of plankton trophic levels (2, 6, 7), whereas others conclude that strong top-down control (8) or weak coupling (9, 10) is operative.

Complicating the identification of processes underpinning marine food web dynamics is a range of methodological limitations: time series of biotic variables tend to be short; spatial coverage of most studies is restricted to point sampling; and syntheses often attempt to combine results from studies with very different field and analytical approaches. We overcome such problems by using 115,322 samples taken by the Continuous Plankton Recorder (CPR) survey in the Northeast Atlantic between 1958 and 2002. These samples have been collected, processed, and analyzed in a consistent manner, yielding reliable time series for ~400 taxa (11) and providing a unique opportunity to investigate planktonic ecology over decadal and ocean basin scales. Using these data, we construct a conceptual pelagic food web

<sup>1</sup>Sir Alister Hardy Foundation for Ocean Science, The Laboratory, Citadel Hill, Plymouth, PL1 2PB, UK. <sup>2</sup>Department of Zoology, University of Port Elizabeth, Port Elizabeth, South Africa.

\*To whom correspondence should be addressed. E-mail: anr@sahfos.ac.uk

comprising phytoplankton (diatoms and dinoflagellates), copepod herbivores, and zooplankton carnivores (see supporting online text for taxonomic membership of functional groups). Because we are interested in ecosystem responses, rather than local or taxon-specific responses as in many previous studies (5, 8, 12, 13), we calculate the total abundance (11) of all species sampled within each of these functional groups (14). We use mean annual sea surface temperature (SST; HadISST Version 1.1 from Hadley Centre, UK Met Office) as an environmental proxy because it is an important manifestation of climate change (4), it is associated with changes in phytoplankton community structure (15), and it is available over the time and space scales necessary for this study (16).

Because of the difficulty of testing hypotheses in the global oceans by conducting in situ manipulative experiments at the scale of the present study, conclusive cause-and-effect evidence of underlying mechanisms is not possible. The comparative approach is often useful in such situations, and we use this method to test ideas concerning the impact of climate change on the plankton community and also to investigate the form and strength of trophic linkages (relationships between functional feeding groups that are adjacent to one another in the conceptual food web) within the plankton. This is achieved by partitioning the Northeast Atlantic into regions based on “standard boxes” used in the survey (Fig. 1). Within these regions we calculate annual mean SST and abundance time series for each trophic level (17) to minimize temporal autocorrelation associated with strong seasonality. We then correlate time series of annual means from different trophic

levels. Strong bottom-up control should result in a positive correlation between predator and prey, strong top-down control should result in a negative correlation between predator and prey, and strong climate control at any level within the food web should result in significant correlations between abundance within a trophic level and some environmental (here SST) variable (13). To identify general patterns, we then use a random-effects meta-analysis (13) to combine individual correlation coefficients across our study domain. We focus on the 20 regions in the Northeast Atlantic that have sufficient data (20 or more years) (Fig. 1) to estimate the temporal autocorrelation functions that are required for adjusting effective degrees of freedom using the modified Chelton Method (18, 19). To minimize potential effects of spatial autocorrelation, we also perform a meta-analysis on a subset of nine noncontiguous regions (A1, A6, B2, C3, C5, D1, D3, E5, and F4—this is the largest possible number of noncontiguous regions that has the longest overall time series). Examination of patterns of covariation in environmental and trophic relationships in pairwise combinations of these nine noncontiguous regions (supporting online text) confirms that their spatial separation allows them to be regarded as replicates.

Correlations between phytoplankton abundance and SST for each of the 20 regions that have sufficient data for analysis are shown in Fig. 2A. We set  $\alpha$  at 0.01 for all analyses to ameliorate the effects of multiple hypothesis tests, so correlations are significant when the 99% confidence intervals do not overlap zero. There is no consistent pattern in the sign of the correlations over the regions, and only two of the individual correlation coefficients are sig-

nificant. Furthermore, neither the meta-analysis for all regions [ $\bar{r}_{All} = 0.12$ ,  $Z = 1.94$ , not significant (n.s.)] nor that for the subset of nine noncontiguous regions ( $\bar{r}_{Subset} = 0.06$ ,  $Z = 0.60$ , n.s.) is significant, suggesting no overall linear relation.

The possibility remains, however, that although the relation between phytoplankton abundance and SST is not consistent throughout the study domain, its strength nevertheless varies in a predictable way (13, 20). To examine this hypothesis, we plot the phytoplankton abundance–SST correlation against mean SST for each region (Fig. 2B) and find a strong negative relation for all areas ( $r = -0.61$ ,  $P < 0.01$ ,  $n = 20$ ) as well as for the subset of noncontiguous areas ( $r = -0.81$ ,  $P < 0.01$ ,  $n = 9$ ). These results imply that the abundance of phytoplankton increases as SST warms in cooler waters of the Northeast Atlantic, but that it decreases as SST increases in warmer waters.

This complex response of phytoplankton abundance to SST probably arises because temperature not only affects biota directly, but also acts as a useful proxy for other physical processes regulating the size structure, taxonomic composition, and abundance of phytoplankton communities (15, 21). For instance, seasonal

**Fig. 1.** Map of the Northeast Atlantic Ocean showing standard CPR boxes (bold) and the number of years (from 1958 to 2002) that eight or more months were sampled within each box (italics). Because of the strong seasonality in plankton populations, annual means were only calculated for years when eight or more months were sampled (17).

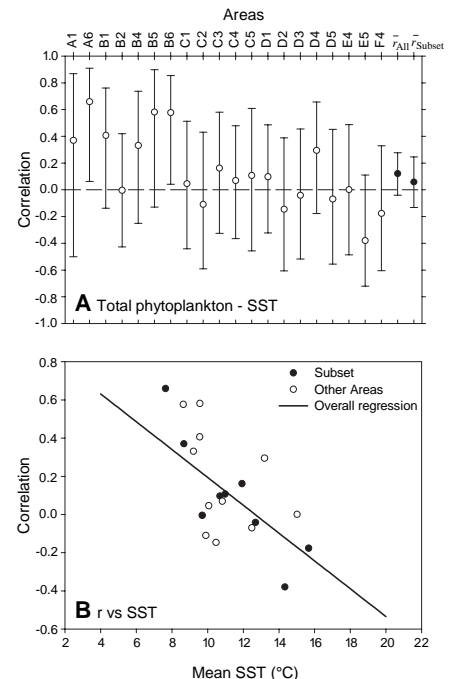
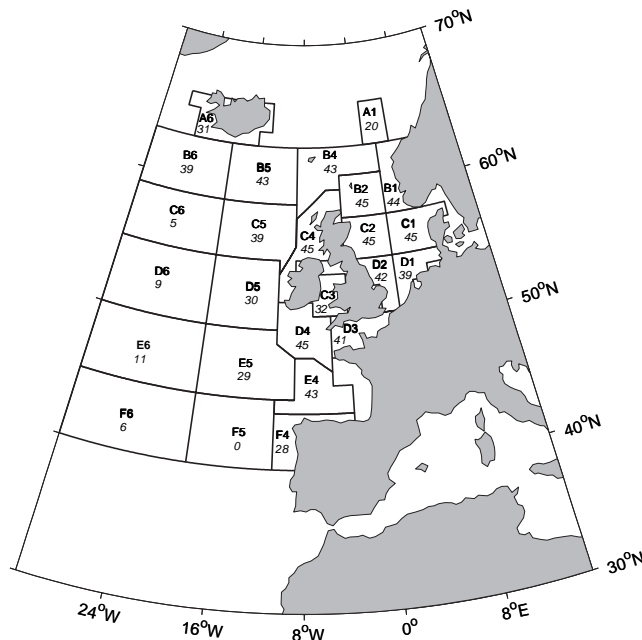


**Fig. 2.** (A) Meta-analysis of the relation between phytoplankton abundance and SST, showing no overall relation. Weighted mean correlations (circles) are shown with 99% confidence limits (bars) calculated using the random-effects model B for the entire study area ( $\bar{r}_{All}$ ) and a subset of nine noncontiguous regions ( $\bar{r}_{Subset}$ ). Bars not overlapping zero are significant. (B) The inverse relation between phytoplankton abundance–SST correlations and mean SST (°C) in each region. Points represent individual regions.

and regional changes in vertical stratification and nutrients are often associated with changes in SST (22, 23). In the Northeast Atlantic, there is also a strong relation between winds and SST, particularly westerly winds (24) that are important for mixing and stratification, a likely consequence of the large-scale atmospheric forcing by the North Atlantic Oscillation (NAO) (25).

The regions in this study generally fall into two turbulence–nutrient regimes associated with temperature (15), namely, turbulent–nutrient–rich cool waters (left side of Fig. 2B) and stratified–nutrient-poor warm waters (right side of Fig. 2B). In cooler waters with relatively strong turbulence and plentiful nutrients, it is likely that warming will boost phytoplankton metabolic rates as well as increase stratification, both processes leading to increased phytoplankton abundance (21). In warmer, more stratified waters with limited nutrients, it is likely that warming may reduce total phytoplankton abundance (at least of large cells), because increased heating can enhance existing stratification (2), reducing the availability of nutrients to phytoplankton and leading to a microbial-dominated community (26). This inverse linear relation between the response of phytoplankton abundance to SST and mean regional SST may therefore hold for large areas of the open ocean and continental shelf.

This does not discount the existence of other oceanographic processes in areas where factors such as salinity can play a dominant role in controlling water-column stability

(15). Examples include areas close inshore where stability is influenced by riverine runoff (stratified–nutrient rich), and polar regions where stability is controlled predominantly by ice melt (turbulent–nutrient poor/high nitrate). However, such areas make up only a tiny fraction of the temperate marine pelagic environment and are not well sampled by the CPR survey, thereby effectively excluding them from our analysis.

To determine whether the climate signal propagates up the plankton food web (bottom-up) or whether grazing by herbivores may impact phytoplankton abundance (top-down), we investigate the link between the abundances of copepod herbivores and their phytoplankton prey. All but one linkage is positive, although most of the correlations are not significant individually (Fig. 3A). The meta-analysis of all regions nevertheless indicates that the overall relation between the abundances of herbivorous copepods and phytoplankton is positive and highly significant ( $\bar{r}_{All} = 0.27$ ,  $Z = 6.41$ ,  $P < 0.0001$ ), with the analysis of the noncontiguous regions verifying this result ( $r_{Subset} = 0.25$ ,  $Z = 3.54$ ,  $P < 0.001$ ). These positive correlations are unlikely to be a consequence of both trophic levels responding directly to SST, because there was no significant relation between copepod herbivore abundance and SST ( $r_{All} = -0.04$ ,  $Z = -0.65$ , n.s.;  $\bar{r}_{Subset} = 0.06$ ,  $Z = 0.60$ , n.s.). These relationships are therefore likely to result from consistent bottom-up control of herbivorous copepods by their phytoplankton prey, although the relatively small correlation coefficients suggest that other factors such as disparities in P/B (production/biomass) ratios between predators and their prey might also be important in this link.

To assess whether the signal propagates as far as secondary consumers, we investigated the link between abundances of zooplankton carnivores and their copepod herbivore prey (Fig. 3B). All correlations are strongly positive and all but one are individually significant. The meta-analysis of all regions confirms that there is a very strong and significant positive relation between abundances of secondary consumers and herbivorous copepods ( $\bar{r}_{All} = 0.72$ ,  $Z = 11.92$ ,  $P < 0.0001$ ), with the analysis of noncontiguous regions supporting this conclusion ( $\bar{r}_{Subset} = 0.79$ ,  $Z = 10.10$ ,  $P < 0.0001$ ). These strong positive correlations are unlikely to be a consequence of both trophic levels responding directly to SST, because there was no significant relation between carnivorous zooplankton abundance and SST ( $\bar{r}_{All} = 0.11$ ,  $Z = 1.63$ , n.s.;  $\bar{r}_{Subset} = 0.12$ ,  $Z = 0.88$ , n.s.). These results suggest that there is close and consistent bottom-up control of carnivorous zooplankton by their herbivorous copepod prey.

By investigating the linkages in the plank-

ton food web at large time and space scales that subsume local variation, meaningful patterns are revealed (21). The magnitude, together with the consistency in form, of the linkages from phytoplankton through copepod herbivores to zooplankton carnivores provides strong support for dominant bottom-up control within the plankton community in the Northeast Atlantic over the time (decades) and space (ten thousands of km<sup>2</sup>) scales of the present study. This contrasts with recent meta-analyses (9, 10), which conclude that linkages within the marine plankton community tend to be weak or inconsistent across trophic levels. The strengths of our study, and hence the value of our results, include its wide spatial and temporal scales, the incorporation of a broad taxonomic diversity in each trophic level, and the uniform sampling methodology through time for all plankton in the different regions.

The present findings suggest a possible mechanism underlying some previously observed relationships between fish ecology and climate. For example, recent work has shown that warmer temperatures in northern areas of the Northeast Atlantic support good cod recruitment, whereas warmer temperatures in areas to the south are detrimental to cod recruitment (27). Moreover, relationships between the NAO and many fish stocks in the Northeast Atlantic (28) may be a consequence of the impact of the NAO on local conditions, such as temperature (24), which then may propagate up the plankton food web.

The tight coupling between the plankton trophic levels in marine pelagic ecosystems over the large time and space scales shown in this study should aid prediction of impacts of future climate change on marine food webs. Over the study period (1958 to 2002), we observed a slight cooling of 0.1°C in some northern areas, but a substantial warming of 0.5°C in the southern regions. Ocean temperatures are likely to be further affected by anthropogenic climate change; the Intergovernmental Panel on Climate Change predicts a rise in temperature of between 2° and 4°C in the northeast Atlantic by 2100, with greater increases in the north than in the south (29). Our findings suggest that any effects of such climate change will have an impact on phytoplankton, copepod herbivores, and zooplankton carnivores, thereby affecting ecosystem services, such as oxygen production, carbon sequestration, and biogeochemical cycling. Although the direct consequences of these changes for fisheries are not clear, it seems inevitable that fish, seabirds, and marine mammals will need to adapt to a changing spatial distribution of primary and secondary production within pelagic marine ecosystems. Given the scales at which our analyses were conducted and the consistency

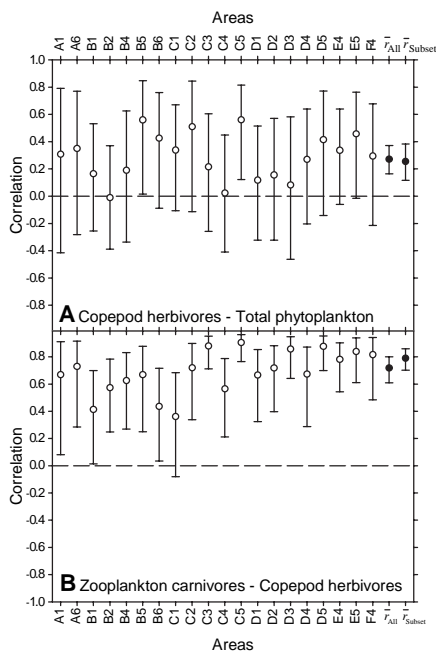


**Fig. 3.** Meta-analysis of trophic linkages suggesting strong bottom-up control of (A) copepod herbivores by phytoplankton and (B) zooplankton carnivores by copepod herbivores. Symbols as in Fig. 2A.

of our results, it is reasonable to expect that our findings may generalize to other mid-latitude marine pelagic ecosystems. Under such a scenario, impacts will undoubtedly be felt not only in the oceans, but also in terrestrial ecosystems globally.

References and Notes

1. P. G. Falkowski, R. T. Barber, V. Smetacek, *Science* **281**, 200 (1998).
2. D. Roemmich, J. McGowan, *Science* **267**, 1324 (1995).
3. L. Hughes, *Trends Ecol. Evol.* **15**, 56 (2000).
4. G. Beaugrand, P. C. Reid, F. Ibañez, J. A. Lindley, M. Edwards, *Science* **296**, 1692 (2002).
5. P. Cury et al., *ICES J. Mar. Sci.* **57**, 603 (2000).
6. N. J. Aebischer, J. C. Coulson, J. M. Colebrook, *Nature* **347**, 753 (1990).
7. X. Irigoien, J. Huisman, R. P. Harris, *Nature* **429**, 863 (2004).
8. G. M. Daskalov, *Mar. Ecol. Prog. Ser.* **225**, 53 (2002).
9. F. Micheli, *Science* **285**, 1396 (1999).
10. J. B. Shurin et al., *Ecol. Lett.* **5**, 785 (2002).
11. P. C. Reid, J. M. Colebrook, J. B. L. Matthews, J. Aiken, *Prog. Oceanogr.* **58**, 117 (2003).
12. G. Beaugrand, K. M. Brander, J. A. Lindley, S. Souissi, P. C. Reid, *Nature* **426**, 661 (2003).
13. B. Worm, R. A. Myers, *Ecology* **84**, 162 (2003).
14. The spatial, temporal, taxonomic, and ecological scales considered here force some simplifications. For example, all abundance estimates in this study represent indices of near-surface plankton abundance and not absolute values, because the CPR is towed at a depth of ~10 m and many taxa, especially smaller ones, are caught only semiquantitatively. We calculate abundance rather than biomass time series for each trophic level because neither mass nor length measurements are taken from CPR samples, so biomass estimates would require additional assumptions. Within the coarse trophic categories in this study, members (supporting online text) are deemed to be generalist feeders, so each is considered a functional group. Although the phytoplankton compartment does not include nanoflagellates (they are too delicate to be preserved on CPR silks), we are primarily interested in phytoplankton as food for herbivorous copepods, and these feed preferentially on the larger phytoplankton. The zooplankton carnivore compartment includes data on siphonophore abundance, but corresponding data for other cnidarians are not available due to damage during sampling. We do not include meroplankton because their dynamics can be heavily influenced by processes independent of the pelagic ecosystem. We also do not include various other functional groups such as picoplankton, fish, birds, or marine mammals because time series are not available at the appropriate scales for our study. Thus, our conclusions can only be applied to groups sampled quantitatively by the CPR and cannot easily be extended to include the entire pelagic ecosystem.
15. H. A. Bouman et al., *Mar. Ecol. Prog. Ser.* **258**, 19 (2003).
16. We do not use wind or hydrographic (current) data because they have differential effects over the study domain. Reliable time series for clouds are rare over the entire study period (1958 to 2002) and domain. We also do not use an integrative environmental index such as the NAO because it does not allow analysis of the direct responses of plankton communities to their local environment, and because the effects of climate change on the NAO are less clearly understood than are those on SST.
17. J. M. Colebrook, *Bull. Mar. Ecol.* **8**, 143 (1975).
18. B. J. Pyper, R. M. Peterman, *Can. J. Fish. Aquat. Sci.* **55**, 2127 (1998).
19. To apply the modified Chelton Method we estimated autocorrelation functions for each time series. Because many were broken, we used a spline smoother to interpolate data for up to two missing years. These interpolated data were used only to determine the number of degrees of freedom to be removed from analyses; in no way were they used to inflate the time series or to alter correlation coefficients.

20. B. Planque, T. Frédo, *Can. J. Fish. Aquat. Sci.* **56**, 2069 (1999).
21. W. K. W. Li, *Nature* **419**, 154 (2002).
22. K. L. Carder, F. R. Chen, Z. P. Lee, S. K. Hawes, D. Kamykowski, *J. Geophys. Res.* **104**, 5403 (1999).
23. S. Sathyendranath, G. Cota, V. Stuart, H. Maass, T. Platt, *Int. J. Remote Sens.* **22**, 249 (2001).
24. J.-M. Fromentin, B. Planque, *Mar. Ecol. Prog. Ser.* **134**, 111 (1996).
25. J. W. Hurrell, *Science* **269**, 676 (1995).
26. D. H. Cushing, *J. Plankton Res.* **11**, 1 (1989).
27. C. M. O'Brien, C. J. Fox, B. Planque, J. Casey, *Nature* **404**, 142 (2000).
28. L. S. Parsons, W. H. Lear, *Prog. Oceanogr.* **49**, 167 (1999).
29. J. T. Houghton et al., Eds., *Climate Change 2001: The Scientific Basis* (Cambridge Univ. Press, Cambridge, 2001).
30. We thank A. Lindley and M. Gibbons for helping us assign zooplankton to functional groups, as well as the Hadley Centre, UK Met Office, for providing the SST data (HadISST Version 1.1) at no cost. D.S.S.

gratefully acknowledges the funding generously provided for this work by the South African National Research Foundation (GUN 2053579), the Ernest Oppenheimer Memorial Trust, and the University of Port Elizabeth, and A.J.R. acknowledges the financial support of Department of Environment Food and Rural Affairs contract MFO430. The CPR survey would not be possible without the cooperation of the agents, owners, masters, and crews of the vessels that tow the recorders. A funding consortium made up of governmental agencies from Canada, France, Iceland, Ireland, the Netherlands, Portugal, the United Kingdom, and the United States financially supports the survey. CPR data are available freely to the international scientific community for research (see www.sahfos.org).

Supporting Online Material

www.sciencemag.org/cgi/content/full/305/5690/1609/DC1  
 SOM Text  
 Table S1  
 References

1 June 2004; accepted 10 August 2004

# Methanobactin, a Copper-Acquisition Compound from Methane-Oxidizing Bacteria

Hyung J. Kim,<sup>1\*</sup> David W. Graham,<sup>1†</sup> Alan A. DiSpirito,<sup>5</sup> Michail A. Alterman,<sup>2</sup> Nadezhda Galeva,<sup>3</sup> Cynthia K. Larive,<sup>4</sup> Dan Asunskis,<sup>6</sup> Peter M. A. Sherwood<sup>6</sup>

Siderophores are extracellular iron-binding compounds that mediate iron transport into many cells. We present evidence of analogous molecules for copper transport from methane-oxidizing bacteria, represented here by a small fluorescent chromopeptide (C<sub>45</sub>N<sub>12</sub>O<sub>14</sub>H<sub>62</sub>Cu, 1216 daltons) produced by *Methylosinus trichosporium* OB3b. The crystal structure of this compound, methanobactin, was resolved to 1.15 angstroms. It is composed of a tetrapeptide, a tripeptide, and several unusual moieties, including two 4-thionyl-5-hydroxyimidazole chromophores that coordinate the copper, a pyrrolidine that confers a bend in the overall chain, and an amino-terminal isopropylester group. The copper coordination environment includes a dual nitrogen- and sulfur-donating system derived from the thionyl imidazolate moieties. Structural elucidation of this molecule has broad implications in terms of organo-copper chemistry, biological methane oxidation, and global carbon cycling.

The mechanisms involved in microbial copper homeostasis are rapidly being elucidated, although the workings of such systems are only understood in model organisms such as *Escherichia coli*, *Enterococcus hirae*, and *Saccharomyces cerevisiae* (1–4). In these organisms, copper homeostatic systems are geared toward active detoxification as op-

posed to accumulation and storage. However, in many methanotrophic bacteria (aerobes that oxidize CH<sub>4</sub> for carbon and energy and play a major role in the global carbon cycle), copper homeostasis differs because copper requirements can be up to fourfold higher than iron requirements (5–7). In such methanotrophs, copper plays a central role in metabolism, regulating expression of two methane monooxygenases: a soluble methane monooxygenase (sMMO) and particulate methane monooxygenase (pMMO) (5, 8–10). Copper also influences the expression of at least two of the four formaldehyde dehydrogenases (11–13), the development of internal membranes (5, 8, 14, 15), and the expression of other polypeptides related to copper regulation or transport (5, 16–19).

Given the notable role of copper in methanotroph physiology, we postulated that these

<sup>1</sup>Department of Civil, Environmental, and Architectural Engineering, <sup>2</sup>Biochemical Research Service Laboratory, <sup>3</sup>Mass Spectrometry Laboratory, <sup>4</sup>Department of Chemistry, University of Kansas, Lawrence, KS 66045, USA. <sup>5</sup>Department of Biochemistry, Biophysics, and Molecular Biology, Iowa State University, Ames, IA 50011, USA. <sup>6</sup>Department of Chemistry, Kansas State University, Manhattan, KS 66506, USA.

\*Present address: Department of Biochemistry, Molecular Biology, and Biophysics, University of Minnesota, St. Paul, MN 55108, USA.

†To whom correspondence should be addressed. E-mail: dwgraham@ku.edu